Chapter 10
Damage Identification on Gear Drivetrains Using Neural Networks Trained by High-Fidelity Multibody Simulation Data

J. Koutsoupakis, D. Giagopoulos, G. Karyofyllas, P. Seventekidis, and S. Natsiavas

Abstract In this work, structural health monitoring of an experimental gear drivetrain is examined by means of machine learning algorithms trained though high-fidelity data, generated by optimal Multibody Dynamics models. The model's accuracy is enhanced through detailed modeling of the contact mechanics in gear meshing, via the development of a novel contact force model dedicated to gears, which accounts for the effects emanating from the time varying mesh stiffness, transmission error and backlash between them. This detailed contact force formulation takes into account the geometry of the gears, allowing for modeling potential asperities in them, such as surface roughness, spalls or missing teeth, which may lead to errors during motion transmission and produce greater damages in a mechanical system. Data is then generated through repetitive simulations of the optimal numerical model, simulating the system's operation in its healthy state as well as in the presence of faults. The produced data is then used to train an ensemble of neural networks for the task of structural health monitoring on the gear drivetrain through analysis of its response in the frequency domain. The trained algorithms are then employed in damage detection and characterization on the physical drivetrain, proving that they can generalize their health state predictions on unknown, real-world data successfully, and validating the proposed structural health monitoring framework of utilizing training data from the numerical domain.

Keywords Time Varying Mesh Stiffness · Backlash · Transmission Error · Nonlinear Dynamics · Machine Learning

Introduction

As awareness regarding the benefits of proper maintenance of machinery increases, the need for timely detection of defects in transmission systems, particularly those used in critical applications such as industrial machinery or vehicles has led to the development of a series of Condition Monitoring (CM) methods. Vibration-based methods in particular have been extensively applied to gear transmission systems due the large amount of information contained in the system's vibration response and the accessibility of data even during operation of a system [1][2][3]. While, traditionally, damage detection would be based on signal analysis tools and fault indices, such as the Root Mean Square (RMS) or kurtosis of a measured signal, as well as the analysis of a system's response from a professional, the rapid increase in Machine Learning (ML) algorithms and tools has provided additional options in the task of CM [4][5][6]. While powerful, as ML methods such Artificial Neural Networks (ANNs) are global approximators, use of such tools requires vast amounts of data, particularly for labeled classification tasks, such as damage detection and characterization, that is, accurately predicting the health state of a mechanical system requires that the ML algorithm has been trained on similar, labeled data. This data, however, is usually scarce or even inexistent, due to the prohibiting cost of extensively instrumenting machinery or, in the case of collecting damaged state data, deliberately causing defects to a machine's components. To mitigate this shortcoming, multiple data augmentation methods can be found in literature [7][8], as a means of producing more samples based on a small number of physical measurements. These data augmentation methods, however, require measurements of every defect of interest, thus not being practical in cases where no data from nominally identical structures and cases is available.

To this end, numerical simulations have been explored as a means of synthetic data generation, where using methods such as Finite Element Modeling (FEM) [9] or Multibody Dynamics (MBD) analysis [10], one can generate a virtually infinite amount of data from models corresponding the different health states of a system. Using this simulation data, algorithms

J. Koutsoupakis · D. Giagopoulos · G. Karyofyllas · P. Seventekidis · S. Natsiavas
Aristotle University of Thessaloniki, Department of Mechanical Engineering, Thessaloniki, GR, 54124
Corresponding author: dgiagopoulos@auth.gr
e-mail: jkoutsoup@meng.auth.gr; gdkaryof@meng.auth.gr; seventep@meng.auth.gr; natsiava@auth.gr

Brian Damiano et al. (eds.), *Structural Health Monitoring & Machine Learning, Vol. 12*, Conference Proceedings of the Society for Experimental Mechanics Series, https://doi.org/10.13052/97887-438-0157-3_10

such as ANNs can be trained in the numerical domain and employed in making predictions in the physical domain, so long as the simulated data hold similar characteristics as those contained in the physical measurements. This similarity between the numerical and physical data is achieved by optimizing the models using a small number of healthy state measurements as well as powerful optimization techniques [11], aiming to minimize an objective function between simulated and real system responses. While this framework has previously been tested, it has become obvious that its capacity is limited by the capacity of the numerical models, that is, especially in cases where machinery is concerned, the MBD models must be able to simulate the various mechanisms of the system with as much accuracy as possible. Gear transmission systems in particular comprise complex mechanisms, where phenomena such as gear meshing dominate the system's response and are usually the key features in a measured signal. Additionally, wear-related faults in gear transmission systems most commonly appear in components such as bearings (inner/outer race defects, etc.), and gears, where cracks or spalls can appear in gear teeth. To accurately model such phenomena, mechanisms such as the Time Varying Mesh Stiffness (TVMS), dynamic error and backlash between gear teeth must be taken into account in the model, aiming to increase the accuracy and fidelity of the results. In this work, a detailed gear meshing force formulation is developed, aiming to achieve high-fidelity simulations where the time varying effects of gear meshing are accurately presented in the numerical model of an experimental gear drivetrain system. The enhanced model, after being properly optimized, is employed in data generation for different health states of the drivetrain, producing the data necessary to train an ensemble of Deep Neural Networks (DNNs) for classifying the physical system's health state.

The rest of this work is structured as follows: First, the theoretical formulation used in this work is described in the Background section. Afterwards the experimental set-up and corresponding MBD models are shown in the Analysis section, where the results of the numerical simulations and damage classification are also presented, aiming to validate the proposed method experimentally. Finally, the findings of this work are discussed in the Conclusions section and further developments are briefly discussed.

Background

The stiffness of a tooth in a meshed gear pair can be broken down to five components based on the potential energy method as [12]:

$$K_h = \frac{\pi EL}{4(1-\nu^2)} \tag{1}$$

$$\frac{1}{K_b} = \int_{-\varphi 1}^{\varphi 2} \frac{3[1 + (\varphi_2 - \varphi)\, sin\varphi cos\varphi_1 - cos\varphi cos\varphi_1]^2\, (\varphi_2 - \varphi)\, cos\varphi}{2EL[(\varphi_2 - \varphi)\, cos\varphi + sin\varphi)]^3} d\varphi \tag{2}$$

$$\frac{1}{K_s} = \int_{-\varphi 1}^{\varphi 2} \frac{1.2\,(1+v)\,(\varphi_2 - \varphi)\, cos\varphi \cos^2\varphi 1}{2EL\,[(\varphi_2 - \varphi)\, cos\varphi + sin\varphi)]} d\varphi \tag{3}$$

$$\frac{1}{K_a} = \int_{-\varphi 1}^{\varphi 2} \frac{(\varphi_2 - \varphi)\, cos\varphi sin^2\varphi 1}{2EL\,[(\varphi_2 - \varphi)\, cos\varphi + sin\varphi)]} d\varphi \tag{4}$$

$$\frac{1}{K_f} = \frac{\cos^2\varphi 1}{EL}[L^*\left(\frac{u_f}{S_f}\right)^2 + M^*\left(\frac{u_f}{S_f}\right) + P^*(1 + Q^*\tan^2\varphi 2)] \tag{5}$$

where K_h, K_b, K_s, K_a and K_f denote the Hertzian, bending, shear, axial and fillet foundation stiffness. The terms E, L and ν are the tooth material modulus of elasticity, the width of the gear tooth and Poisson's ratio respectively and φ_1 and φ_2 are explained schematically in Figure 1. Last, the rest of the terms of Equation (5) are derived from [13].

Note that the Line of Action (LoA) is estimated as the tangent between the two gear base circles. As such, depending on the number of gear teeth, the potential energy method may lead to an over or underestimation of the meshing stiffness. To take this error into account, the meshing stiffness estimation must be split to two cases, based on the minimum number of teeth in a gear, which can be estimated as:

$$z_{min} = 2h_a/\sin^2 a \tag{1}$$

where $h_a$is the addendum of the gear and a is the nominal pressure angle of the gear. The distinction between the two cases can also be achieved by estimating the root and base radii of the gear as:

$$R_B = \frac{mzcosa}{2} \tag{2}$$

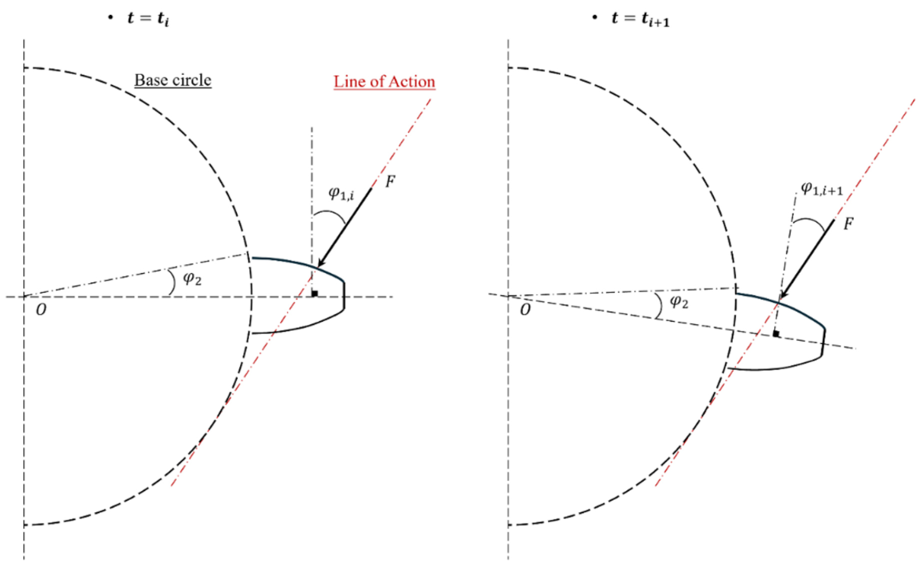

Fig. 1 Cross-section of a gear tooth profile.

$$R_R = \frac{mz}{2} - (h_a + c_n)\, m \tag{3}$$

where m is the normal module, and c_n is the tip clearance coefficient. Depending on the actual teeth in a gear, the stiffness components can be estimated as:

Case 1: $z < z_{min}$

$$\frac{1}{K'_b} = \frac{1}{K_b} + \int_{\varphi 2}^{\varphi 3} \frac{3[1 + (\varphi_2 - \varphi)\, sin\varphi cos\varphi_1 - cos\varphi cos\varphi_1]^2\, (\varphi_2 - \varphi)\, cos\varphi}{2EL[(\varphi_2 - \varphi)\, cos\varphi + sin\varphi)]^3} d\varphi \tag{4}$$

$$\frac{1}{K'_s} = \frac{1}{K_s} + \int_{\varphi 2}^{\varphi 3} \frac{1.2\,(1 + v)\,(\varphi_2 - \varphi)\, cos\varphi \cos^2\varphi 1}{2EL\,[(\varphi_2 - \varphi)\, cos\varphi + sin\varphi)]} d\varphi \tag{5}$$

$$\frac{1}{K'_a} = \frac{1}{K_a} + \int_{\varphi 2}^{\varphi 3} \frac{(\varphi_2 - \varphi)\, cos\varphi sin^2\varphi 1}{2EL\,[(\varphi_2 - \varphi)\, cos\varphi + sin\varphi)]} d\varphi \tag{6}$$

Case 2: $z \geq z_{min}$

$$\frac{1}{K'_b} = \frac{1}{K_b} - \int_{-\varphi 3}^{\varphi 2} \frac{3[1 + (\varphi_2 - \varphi)\, sin\varphi cos\varphi_1 - cos\varphi cos\varphi_1]^2\, (\varphi_2 - \varphi)\, cos\varphi}{2EL[(\varphi_2 - \varphi)\, cos\varphi + sin\varphi)]^3} d\varphi \tag{7}$$

$$\frac{1}{K'_s} = \frac{1}{K_s} - \int_{-\varphi 3}^{\varphi 2} \frac{1.2\,(1 + v)\,(\varphi_2 - \varphi)\, cos\varphi \cos^2\varphi 1}{2EL\,[(\varphi_2 - \varphi)\, cos\varphi + sin\varphi)]} d\varphi \tag{8}$$

$$\frac{1}{K'_a} = \frac{1}{K_a} - \int_{-\varphi 3}^{\varphi 2} \frac{(\varphi_2 - \varphi)\, cos\varphi sin^2\varphi 1}{2EL\,[(\varphi_2 - \varphi)\, cos\varphi + sin\varphi)]} d\varphi \tag{9}$$

This error in the estimated stiffness is better explained in Figure 2, where the relation between angles $\varphi_2,\ \varphi_3$ as well as between the base and root circles is shown.

For a single tooth pair contact, the stiffness can be estimated based on Equations (1) - (9) as:

$$K_{STP} = \frac{1}{\frac{1}{K'_{h,i}} + \frac{1}{K'_{b,i}} + \frac{1}{K'_{s,i}} + \frac{1}{K'_{a,i}} + \frac{1}{K_{f,i}}} \qquad with\ i = 1, 2 \tag{10}$$

Similarly, for the case where more than one gear tooth pair is in contact, the meshing stiffness can be estimated as:

$$K_{MTP} = \frac{1}{\frac{1}{K'_{h,i,j}} + \frac{1}{K'_{b,i,j}} + \frac{1}{K'_{s,i,j}} + \frac{1}{K'_{a,i,j}} + \frac{1}{K_{f,i,j}}} \qquad with\ i = 1, 2\ \&\ j = 1, 2,\ \ldots N \tag{11}$$

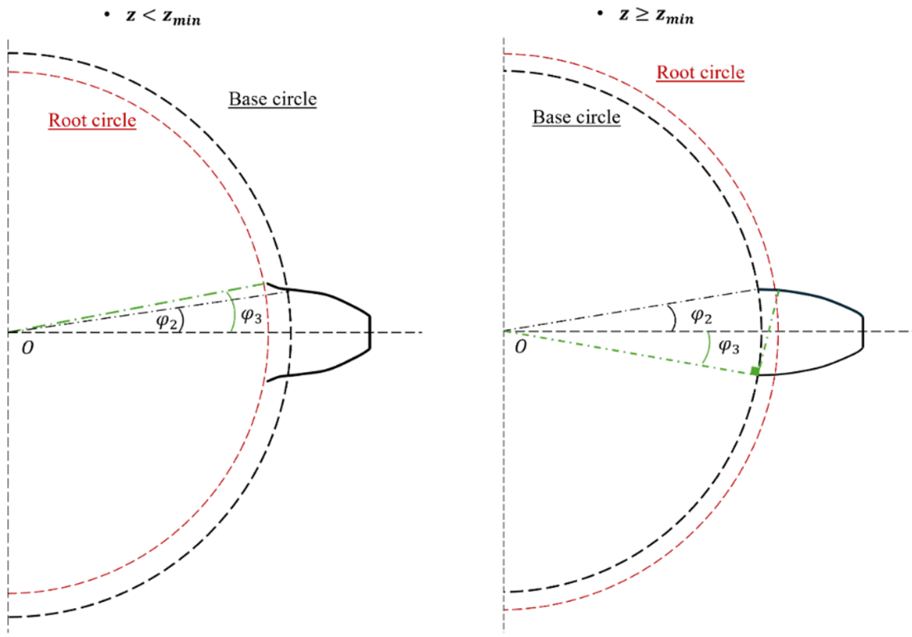

Fig. 2 Cross-section of a gear tooth profile.

Here, the subscript i denotes the pinion (1) and driven (2) gear and j denotes the tooth pair up to N meshed tooth pairs.

In literature, there is a multitude of models which can be used to estimate the normal force between to contacting bodies, such as two gears in mesh. The general expression of the contact normal force is given as:

$$F_N = K\delta^n + \chi\delta^n\dot{\delta} \tag{12}$$

where K denotes stiffness, δ and $\dot{\delta}$ are the indentation depth between the contacting bodies and the respective indentation velocity, n is the nonlinear exponent and χ is the hysteresis damping coefficient which, based on the formulation used, is given in Table 1. In the equations shown in the table, c_r is the coefficient of restitution.

The formulation described in Equations (1) - (11) describes the TVMS for spur gears, where the contact angle is constant for the whole width of a gear tooth. In helical gears, however, due to the helix angle of the gear teeth, the contact angle changes along the width of the gear teeth. To account for this, the slicing method is used to split the gear tooth into subsections and the stiffness is estimated for each slice individually [12]. Then, the total stiffness of a tooth pair can be estimated as the sum of the individual slice stiffnesses as:

$$K_{tot} = \sum_{i=1}^{M} K_i \tag{13}$$

where K_i denotes the stiffness of each slice.

Table 1 Hysteresis damping factor χ with respect to the contact force model.

Gharib & Hurmuzlu	**Herbert & McWhannel**	**Flores et al.**	**Lee & Wang**
$\frac{1}{c_r}\frac{K}{\dot{\delta}^{(-)}}$	$\frac{6(1-c_r)}{(2c_r-1)^2+3}\frac{K}{\dot{\delta}^{(-)}}$	$\frac{8(1-c_r)}{5c_r}\frac{K}{\dot{\delta}^{(-)}}$	$\frac{3(1-c_r)}{4}\frac{K}{\dot{\delta}^{(-)}}$
Hunt & Crossley	**Lankarani & Nikravesh**	**Zhiuing & Qishao**	**Gonthier et al.**
$\frac{3(1-c_r)}{2}\frac{K}{\dot{\delta}^{(-)}}$	$\frac{3(1-c_r^2)}{4}\frac{K}{\dot{\delta}^{(-)}}$	$\frac{3(1-c_r^2)e^{2(1-c_r)}}{4}\frac{K}{\dot{\delta}^{(-)}}$	$\frac{1-c_r^2}{c_r}\frac{K}{\dot{\delta}^{(-)}}$

Aiming to improve the accuracy of the MBD model developed on this work, the Covariance Matrix Adaptation Evolution Strategy (CMAES) was employed. The CMAES algorithm is a powerful population-based method, which is well suited for optimization of non-linear problems, such as the one tackled in this work [9][10][11]. The objective function used in this work is formulated as:

$$J\left(\underline{\theta}\right) = \sum_{i=1}^{M} \sqrt{\sum_{j=1}^{N} \left(\hat{y}_{ij}\left(\underline{\theta}\right) - y_{ij}\right)^2} \tag{14}$$

where $\hat{y}_{ij}\left(\underline{\theta}\right)$ and y_{ij} denote the frequency responses of the numerical and experimental acceleration data respectively, $\underline{\theta}$ denotes the vector containing the contact force related parameters. The subscripts i, j correspond to the measurement location and data point respectively.

In this work, health state classification is achieved in an automated manner by utilizing an ensemble of Deep Learning (DL) classifiers, namely Convolutional Neural Networks (CNNs), trained on data generated from the optimal MBD models of the system in its healthy and damaged states. The trained network ensemble is capable of making predictions on the health state of the physical drivetrain due to the fact that the numerical data is provided through high-fidelity, optimal MBD models, as well as due to the powerful feature extraction capabilities of the convolutional layers. This method of health state classification is presented in the flowchart of Figure 3.

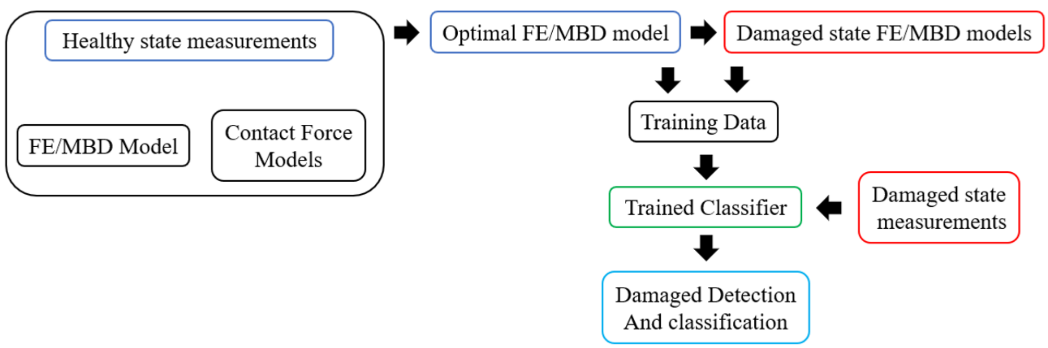

Fig. 3 Numerical data-based ANN training and health state classification method.

Analysis

The experimental system examined in this work is the single stage helical gear transmission system which is shown in Figure 4. The shafts are mounted on the gearbox via deep groove ball bearings while the gears are fixed on the shafts using a screw-wedge mechanism. The gearbox cap is made out of plexiglass, allowing for viewing the gears during operation. Two electric motors are used in the system, comprising the drive and load motors at the inlet and outlet of the setup respectively. The characteristics of the gears used in the experimental setup are explained in detail in Table 2. Experiments were conducted for three inlet velocity values, namely 450, 775 and 1100 RPM, with the load at the outlet shaft kept constant at 10 Nm. Two triaxial accelerometers, denoted as A1 & A2, were placed on the gearbox, above the inlet and outlet shafts respectively, and measurements were extracted with a sampling frequency of 5120 Hz.

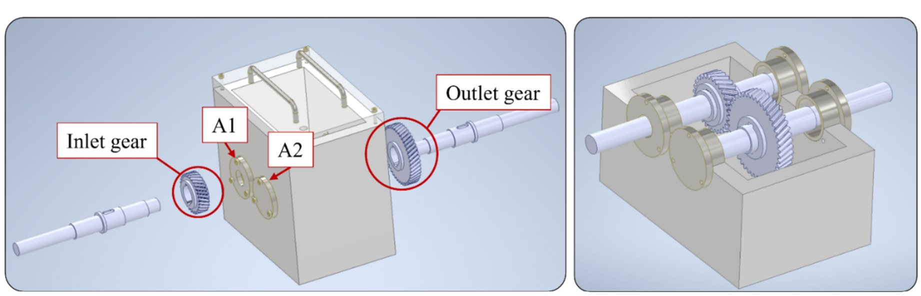

Fig. 4 Single stage helical gear transmission system.

Table 2 Gear geometry related parameters.

Gear	Inlet	Outlet
Module *[mm]*	2.25	2.25
Number of teeth [−]	29	44
Pitch Diameter [mm]	72.7	110.3
Pressure angle [deg]	20	20
Helix angle [deg]	26	26
Helix hand [-]	R	L

The corresponding MBD model of the single stage gearbox is shown in Figure 5.

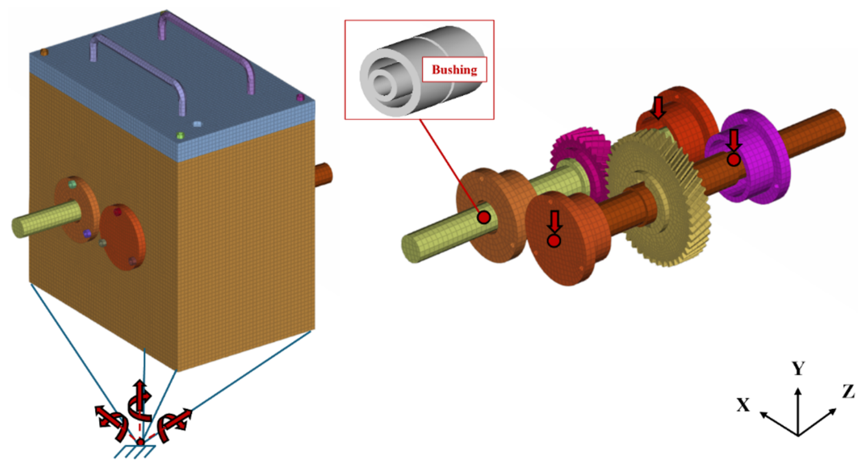

Fig. 5 Single stage helical gear transmission system – MBD model.

A spring-damper force is used to simulate the stiffness at the bolted joints at the base of the gearbox, while the shafts are connected to the gearbox through bushing forces, used as a simplified means of modeling bearings. While this does not allow for modeling the precise bearing dynamics, it was sufficient for the present work, where gear-related phenomena are of interest. Last, the gears are considered fixed to the shafts and a contacting force is acting between them. A constant velocity profile is used as an input to the model while a torque acts on the outlet shaft, simulation the load at the end of the gearbox.

Following the optimization process described in the theoretical background section, the model was optimized based on the healthy state acceleration measurements of the gearbox. The parameters used in the optimization process were the elastic modulus of the gears, assumed equal for both gears, the contact force model (Table 1), the coefficient of restitution and the nonlinear exponent. The final contact stiffness value was estimated based on the Hertzian stiffness formula Equation (1). The updated values for these parameters are shown in Table 3. It should be noted that the parameters of the bushings used in the shafts as well as the spring-damper component that was used to connect the gearbox to the ground could have also been included in the optimization but were omitted for the sake of speeding up the process. This is due to the fact that population-based methods, such as the CMAES algorithm used in this work, require a large number of instances/population for each iteration, which increases as the number of model parameters increases. For these components, nominal values were derived from literature, based on properties used in similar applications, and were then fine-tuned manually, ensuring the final model yielded realistic results.

Table 3 Optimal model and parameters.

Contact force model	$E\ [\frac{N}{mm^2}]$	$c_r[-]$	$n\ [-]$
Lankarani & Nikravesh	2.08e5	0.95	2.13

Figure 6 shows a comparison between the experimental and optimal MBD frequency responses of the single stage drivetrain, measured at the Y axis of accelerometer A. As shown, while both systems display peaks at the orders corresponding to the Gear Mesh Frequency (GMF) and its harmonics, there are some visible differences in the magnitude of the vibrations. Considering that the model was optimized based on the healthy response of the system, this difference in the two responses can be attributed to the limitations imposed due to the modeling of the contact mechanism in the numerical model. That is, while the MBD takes into account phenomena such as the varying backlash between gear teeth as well as the geometry of the tooth, the contact normal force model does not account for the TVMS between gear teeth.

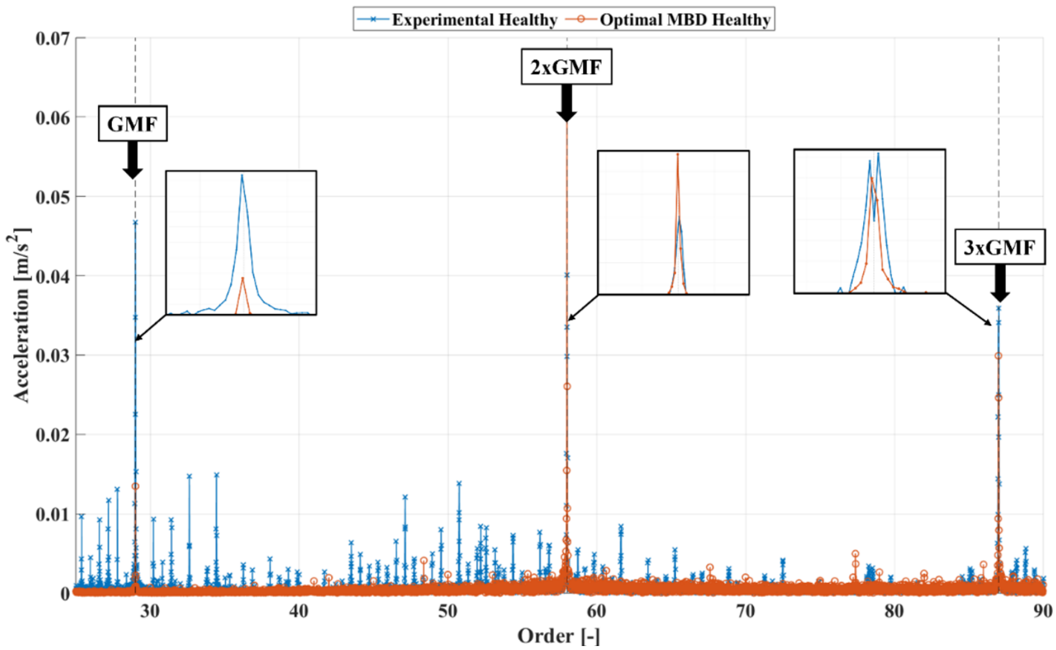

Fig. 6 Frequency response comparison between the experimental and optimal MBD system in its healthy state at 775 RPM.

Aiming to include the effects of TVMS in the MBD model, an augmented contact normal force model was constructed based on the formulation of Equations (1) - (12). By combining this detailed stiffness formulation with the MBD model, the contact forces between gear teeth can be estimated with increased accuracy, as the effects of the varying stiffness due to the changes in the contact angle are taken into account in addition to the force being estimated for infinitely small slices of the gear teeth, due to the contact detection algorithm that is built-in in the MBD model. The operations used in this augmented contact normal force model are described in Algorithm 1, and the stiffness profile resulting from the TVMS formulation is shown in 7.

Algorithm 1. Gear contact normal force algorithm.

- At time t_j, simulation step j:

Step 1. Detect contact between gear teeth at points $\boldsymbol{loc_i},\ i = 1:N$
For $\boldsymbol{loc}$ in $\boldsymbol{loc_i}$:

Step 2. Calculate the angle φ between the LoA and the normal to tooth surface at $\boldsymbol{loc}$

Step 3. Calculate the mesh stiffness $\mathbf{K}$ at $\boldsymbol{loc}$ using Equation (10)

Step 4. Calculate the normal force $\mathbf{F}_{N,i}$ at $\boldsymbol{loc}$ using Equation (12)

Step 5. *Return* $\mathbf{F}_N = \sum_{i=1}^{N} \mathbf{F}_{N,i}$

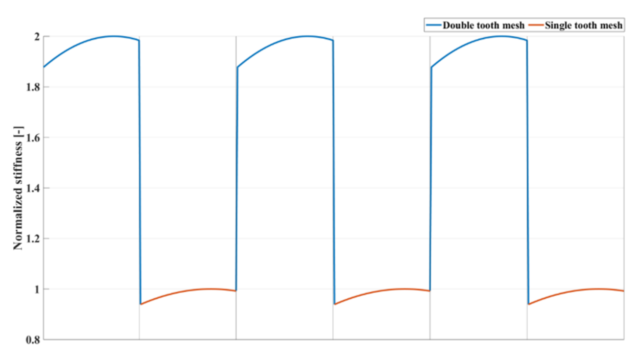

Fig. 7 Time Varying Mesh Stiffness profile.

The effects of the TVMS model are shown in Figure 8 where comparison between the measured and simulated responses is shown for the Y axis of Accelerometer A1.

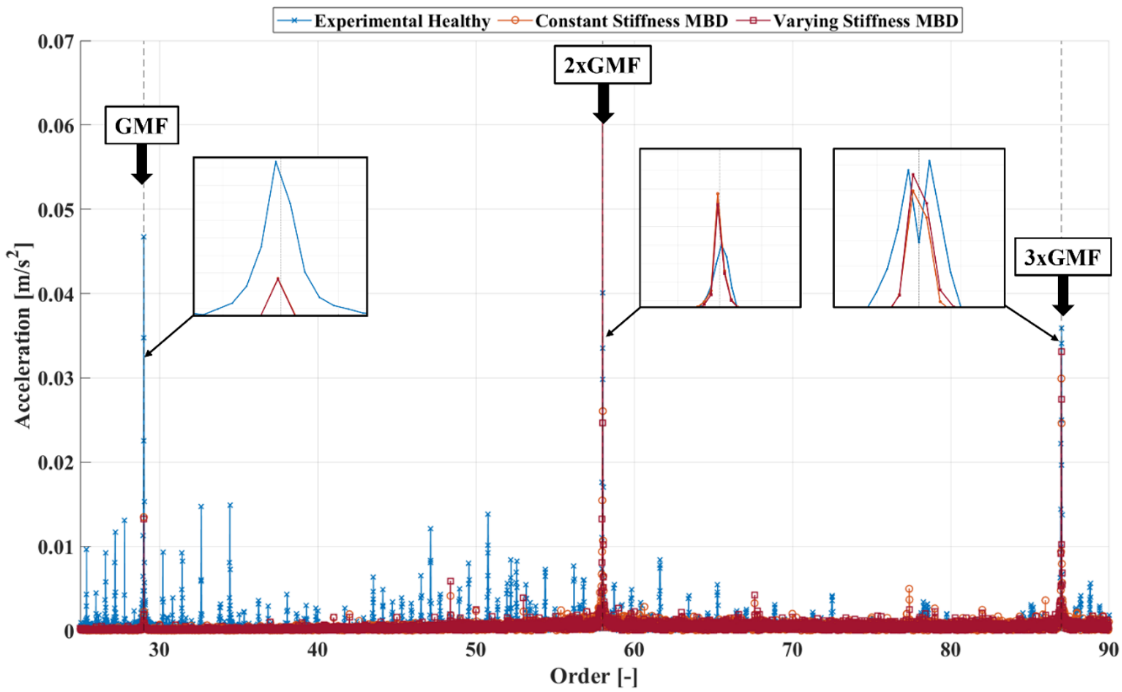

Fig. 8 Comparison between the experimental and the constant and varying stiffness MBD models of the system in its healthy state at 775 RPM.

In this work, two defects were examined to validate the modeling and CM framework. The first case, which for the rest of this text is denoted as Damage 1 (D1), is that of a missing tooth on the inlet gear. The second case, henceforth denoted as Damage 2 (D2) is that of a surface defect on one of the gear teeth. The respective fault cases are shown in Figure 9.

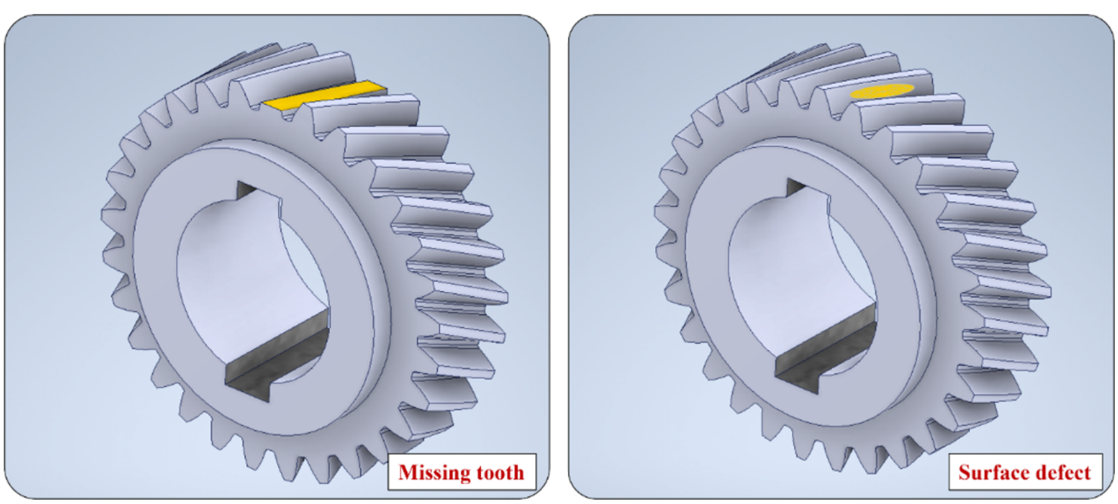

Fig. 9 Experimental drivetrain defective gear cases.

The results from analysis of the system through the MBD simulations of the two damaged gear cases are shown in Figure 10. As indicated by the figure, the damages result in changes in the magnitudes of the GMF and its harmonics, a change in the features of the signal that the DL classifier is expected to be able to identify with great accuracy.

While the results from the optimal MBD simulations in the healthy state of the system indicate a high fidelity between the simulated and measured system responses, validating the proposed numerically trained – experimentally validated CM

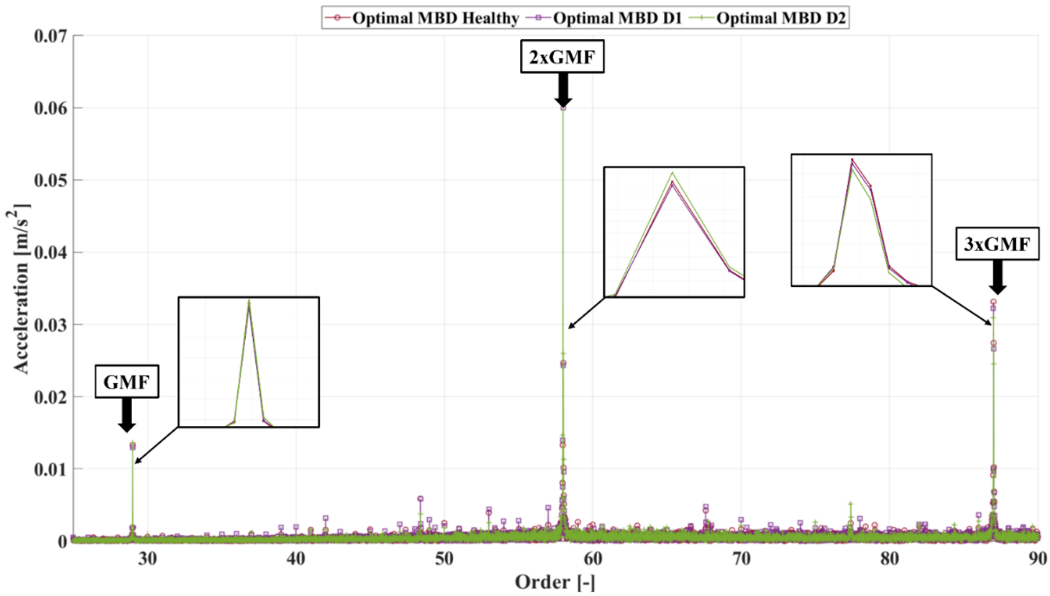

Fig. 10 Comparison between the optimal MBD frequency responses of the three health states at 775 RPM.

framework requires that the DL algorithms are proven capable of generalizing their predictions on unseen, physical measurements. To this end, an ensemble of 10 CNNs is created for the task of multiclass classification. The CNNs, whose architecture is shown in Figure 11, were trained for 25 epochs, on 2000 samples for each health state of the system, generated from the optimal MBD models. The loss function used in the training process was the categorical cross entropy and the optimizer selected was Adam, with a learning rate of 0.002.

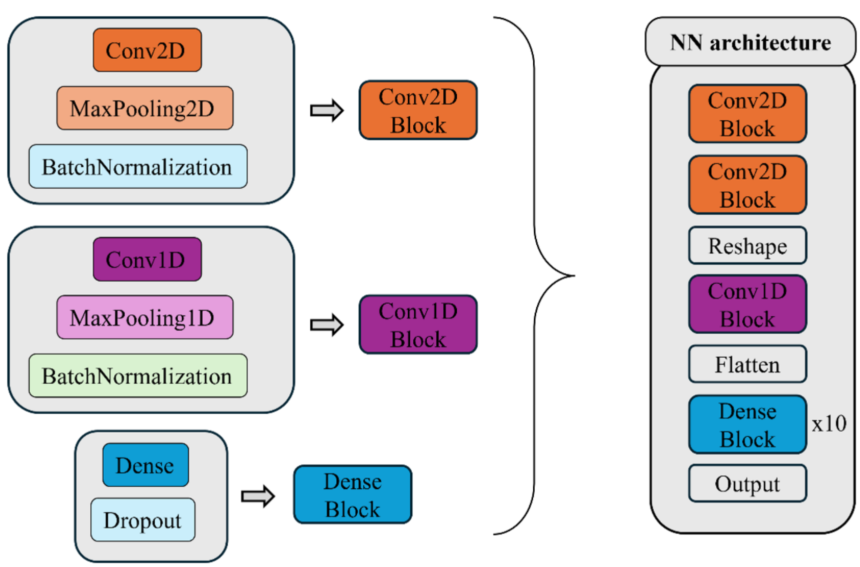

Fig. 11 DL classifier architecture – CNN ensemble.

The CNN ensemble was tested against a total of 300 experimental samples, corresponding to 100 samples for each of the health states. The health state classification results, which are shown in Figure 12, indicate a high level of accuracy and robustness in the predictions of the CNN ensemble. The networks are proven capable of making accurate predictions for each of the three different operating velocity values. Here, it should be noted that the networks are always capable of identifying the D1 case, that is, the missing tooth one, due to the fact that its much more extensive a defect compared to the surface defect. Similarly, most misclassification errors are observed between the healthy and D2 states, where the surface fault is not as extensive and, as such, affects the system's response much more subtly.

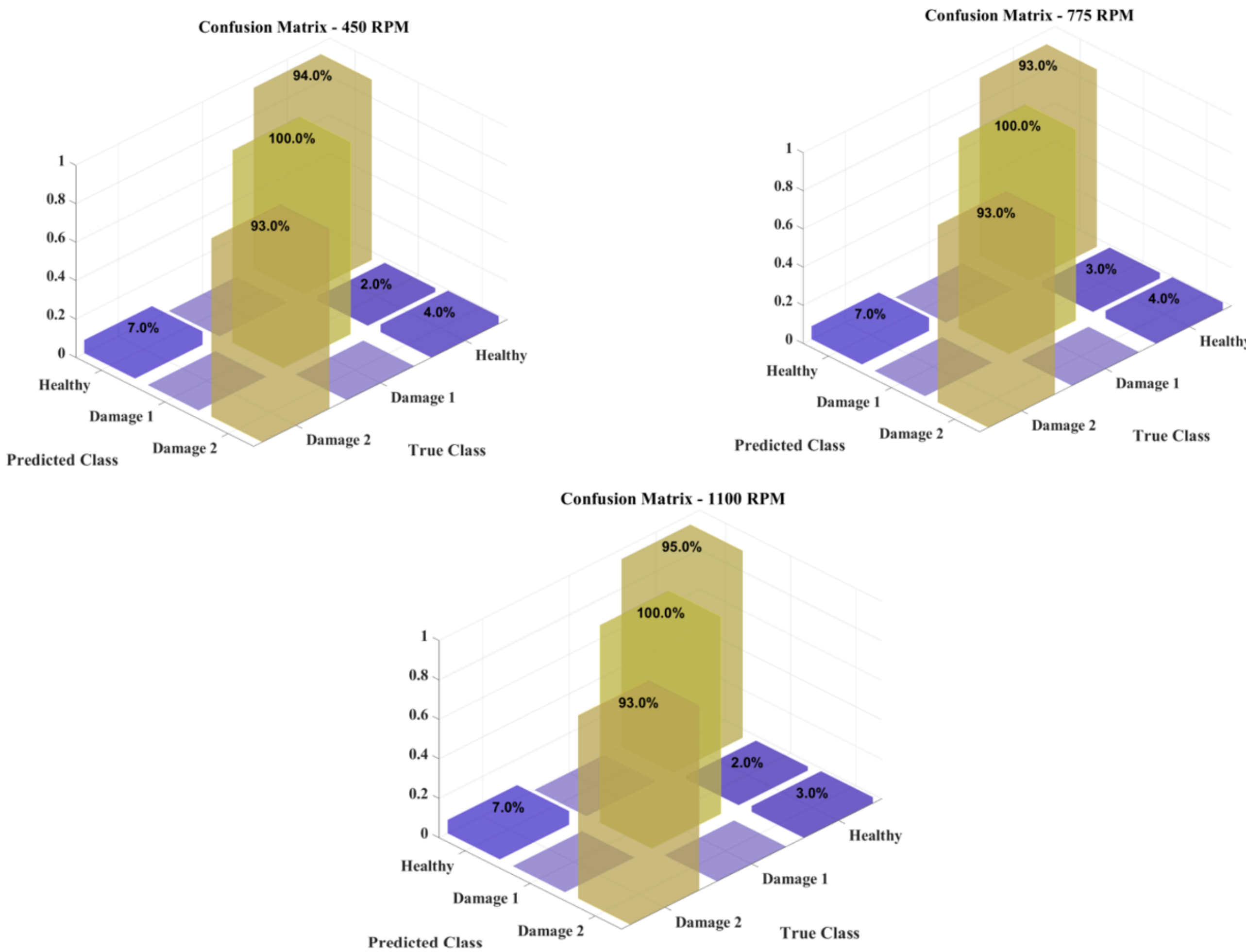

Fig. 12 Health states classification results for the experimental single stage gear drivetrain.

Conclusion

In this work, an augmented optimal MBD model of a single stage gear drivetrain is developed in order to create high-fidelity data for training an ensemble of DL classifiers for CM on the corresponding physical system. This augmented model incorporates an advanced contact normal force module, dedicated to gear meshing, where the effects of the TVMS are taken into account during simulation. This formulation, which is proven to yield improved results compared to the constant stiffness modeling of the contact forces between gears, results in highly accurate numerical data, whose features indicate increased similarity with the physical system's measured response. The developed CNN ensemble which is trained on numerical data alone is proven capable of making accurate predictions of the system's health state, while its robustness is also validated through its application on three different operating velocity conditions. The results derived from this work indicate that modeling mechanisms such as contacts, which are dominant in gear-related applications, with greater detail can significantly improve the simulation accuracy, aiding in the development and improvement of simulation-based DL methods.

Acknowledgments This project is carried out within the framework of the National Recovery and Resilience Plan Greece 2.0, funded by the European Union – NextGenerationEU (Implementation body: HFRI). Project Code: 16381.

References

1. Yuanning Mao, Jun Tong, Zhan Yie Chin, Pietro Borghesani, Zhongxiao Peng, Transmission-error- and vibration-based condition monitoring of gear wear with contaminated lubricant, Wear, Volume 523, 2023, 204760, https://doi.org/10.1016/j.wear.2023.204760.

2. Ke Feng, J.C. Ji, Qing Ni, Michael Beer, A review of vibration-based gear wear monitoring and prediction techniques, Mechanical Systems and Signal Processing, Volume 182, 2023, 109605, https://doi.org/10.1016/j.ymssp.2022.109605.
3. Miljković, Dubravko. (2015). Brief Review of Vibration Based Machine Condition Monitoring. CrSNDT Journal. 5. 14–23.
4. Zhuang Ye, Jianbo Yu, Deep morphological convolutional network for feature learning of vibration signals and itsapplications to gearbox fault diagnosis, Mechanical Systems and Signal Processing, Volume 161, 2021, 107984.
5. R.-B. Sun, Z.-B Yang, L.-D. Yang, B.-J Qiao, X.-F. Chen, K. Gryllias, Planetary gearbox spectral modeling based on the hybrid method of dynamics and LSTM, Mechanical Systems and Signal Processing, Volume 138, 2020,106611.
6. Moslem Azamfar, Jaskaran Singh, Inaki Bravo-Imaz, Jay Lee, Multisensor data fusion for gearbox fault diagnosis using 2-D convolutional neural network and motor current signature analysis, Mechanical Systems and Signal Processing, Volume 144, 2020, 106861.
7. A. L. Marra, R. Juliani and C. Garcia, "Data Augmentation for Vibration Signals using System Identification Techniques," 2021 5th International Conference on System Reliability and Safety (ICSRS), Palermo, Italy, 2021, pp. 281–285, doi:10.1109/ICSRS53853.2021.9660628
8. Timo Koenig, Luca Cadau, Fabian Wagner, Markus Kley, A generative adversarial network-based data augmentation approach with transient vibration data, Procedia Computer Science, Volume 225, 2023, Pages 1340–1349, ISSN 1877–0509, https://doi.org/10.1016/j.procs.2023.10.122.
9. P. Seventekidis, D. Giagopoulos, A. Arailopoulos, O. Markogiannaki, Structural Health Monitoring using deep learning with optimal finite element model generated data, Mechanical Systems and Signal Processing, Volume 145, 2020.
10. Koutsoupakis, J., Seventekidis, P., Giagopoulos, D. (2022). Machine Learning-Based Condition Monitoring with Multibody Dynamics Models for Gear Transmission Faults. Data Science in Engineering, Volume 9 (pp. 51–59). Springer International Publishing.
11. D. Giagopoulos, A. Arailopoulos, Computational framework for model updating of large scale linear and nonlinear finite element models using state of the art evolution strategy. Computers & Structures, 2017. 192: p. 210–232
12. Hongbo Yang, Wenku Shi, Zhiyong Chen, Niancheng Guo, An improved analytical method for mesh stiffness calculation of helical gear pair considering time-varying backlash, Mechanical Systems and Signal Processing, Volume 170, 2022, 108882, https://doi.org/10.1016/j.ymssp.2022.108882.
13. P. Sainsot, P. Velex, O. Duverger, Contribution of gear body to tooth deflections-A new bidimensional analytical formula, J. Mech. Des. 126 (2004) 748–752.